Research Article

SOHAG JOURNAL OF SCIENCES

https://doi.org/ 10.21608/sjsci.2025.396659.1283

# Geomagnetic prospection of the Ptolemaic tombs in Al Dyabat archaeological hill, Akhmim city, Sohag, Egypt

Abdelabaset M. Abudeif *, Mohammed A. Mohammed, and Hossameldeen A. Gaber

*Geology departement, Faculty of science, Sohag University*
**Email: a.abudeif @science.sohag.edu.eg*

**Received:** 22th June 2025 **Revised:** 18th July 2025 **Accepted:** 23th July 2025
**Published online:** 5th September 2025

**Abstract**: This study employs high-resolution magnetic surveying to prospect buried archaeological features, primarily Ptolemaic tombs, within the archaeological hill at Al Dyabat, near Akhmim City, Sohag, Egypt. Despite its historical importance, the site remains largely uninvestigated, presenting a valuable opportunity for new archaeological discoveries. A dual-sensor Overhauser magnetometer was used to conduct a magnetic survey over an area of approximately 2500 m², aiming to detect subsurface anomalies indicative of tomb structures. Advanced data processing techniques, including high-pass filtering, vertical derivatives, analytic signal transformation, Source Parameter Imaging (SPI), and Euler Deconvolution, were applied. The results revealed several shallow magnetic anomalies, ranging in shape from circular to elongated which were interpreted as ninteen potential tombs and associated mudbrick enclosures. These features were identified at depths between 0.5 and 1.5 meters, as outcomed by both SPI and Euler depth solutions. The study demonstrates the effectiveness of jointing magnetic methods in non-invasive archaeological prospection and provides essential guidance for future targeted excavations.

**Keywords:** Magnetic survey, magnetic filtering, Archaeology, Akhmim, Ptolemaic tombs, Non-invasive archaeology.

## 1. Introduction

Akhmim in Upper Egypt is one of the most prominent archaeological cities in Egypt, though there are many more. This ancient city has a rich historical legacy, with extensive cemeteries that date back to the 6th Dynasty of the Old Kingdom (around 2325–2150 BCE) and continued to be used up until the late Coptic period [1]. These burial grounds reflect centuries of continuous occupation and religious significance. Excavations at Akhmim have uncovered a wide array of archaeological treasures, including well-preserved textiles, pottery, tools, and religious artifacts spanning different historical eras. The diversity of findings highlights the city's enduring cultural and spiritual importance throughout ancient Egyptian history. Akhmim was also a prominent religious center, particularly devoted to the fertility god Min [2]. The city's archaeological wealth provides vital insights into the evolution of Egyptian society, art, and burial practices across millennia [3].

Geophysical techniques are highly effective in identifying the locations of buried objects and features at archaeological sites. Traditional exploration techniques, such as trenching and drilling, often demand significant human effort and incur high costs. Additionally, these conventional methods can be destructive to the archaeological context [4].

In archaeological investigations, geophysicists often prioritize the magnetic method before utilizing other geophysical techniques due to its notable effectiveness. This method is particularly advantageous for identifying a wide range of archaeological features, especially those constructed from mudbrick and fired brick, which are typically found at shallow depths. The reliability and accuracy of magnetic surveys in detecting such structures have been well-documented in numerous studies across Egypt. Several researchers have reported the successful application of this technique [5-20]. In sohag area, several authers used magnetic method for archaeological prospection such as Abudeif et al., [5, 6, 8] in Abydos archaeological site. They applied magnetic technique in addition to GPR to locate significant archaeological features within their study sites.

The main objective of this study is to identify and map potential archaeological remains buried at shallow depths within the Al Dyabat archaeological hill, located in Akhmim city, Egypt. A key focus is the detection of Ptolemaic tombs, which vary in form; some being rock-cut, while others are built as brick-lined graves [3]. The area is largely unexplored, with minimal previous archaeological findings, making it a promising site for new discoveries. To achieve this goal, we employed the magnetic method, which has demonstrated effectiveness in numerous archaeological investigations both in Egypt and internationally. The results of this study are expected to support archaeologists in reconstructing the site's layout and in locating additional tombs or structures that are not visible on the surface.

The selected study site is located in Al Dyabat archaeological hill, East of Akhmim city, Sohag Governorate, Egypt. It is located between latitudes 26° 35' 37"N to 26° 35' 39"N, and longitudes 31° 47' 30"E to 31° 47' 33"E (Fig.1).

This archaeological hill is bordered by agricultural land to the west and by El Kawther City to the east. To the north lies the Monastery of the Martyrs, while the Monastery of Saint Mary

the Virgin is situated to the south. The site has been officially recognized as an archaeological area by the Egyptian Ministry of Tourism and Antiquities since February 2018, following the significant discovery of the tomb of the priest Tutu [21], which dates back to the Ptolemaic era. The area contains numerous indications of tombs, either carved into the clay and marl layers or constructed from mudbrick (Fig.2).

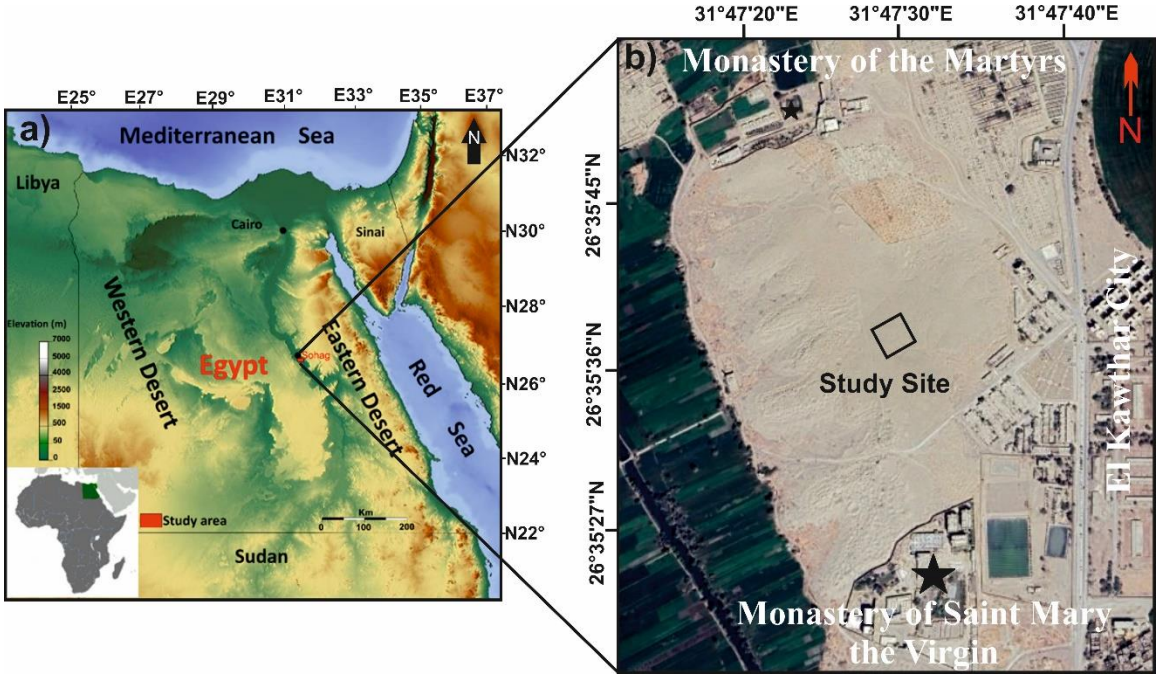


**Figure 1:** A) General location map of Akhmim City, Sohag, B) Landsat image showing the location of study site and its surroundings.

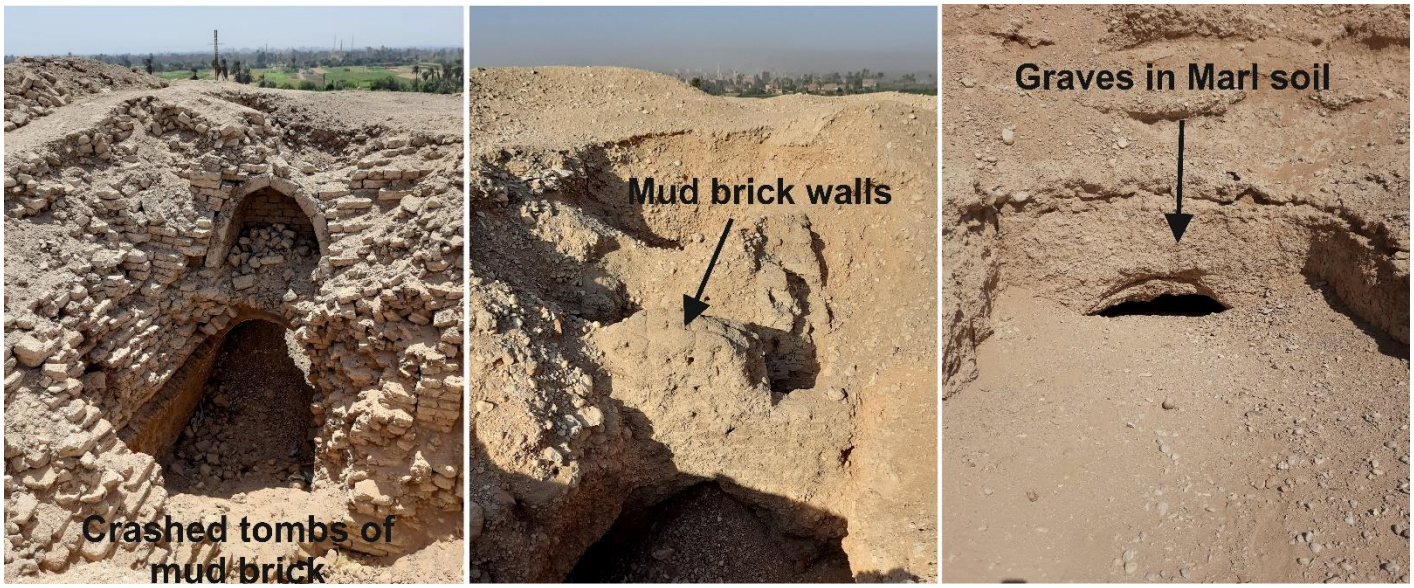


**Figure 2:** Field photographs of near-surface geological and archaeological features in the study area.

## 2. Geological Setting

The East Sohag region in Upper Egypt displays a sequence of stratigraphic units ranging from oldest to youngest, starting with the Lower Eocene formations and progressing upward through the geological time scale to the Holocene deposits. These formations reflect various depositional environments, ranging from shallow marine setting to fluvial, alluvial and lacustrine systems (Fig. 3).

### 2.1. The Drunka Formation (Lower Eocene).

The Drunka Formation, overlies the Thebes Formation, consists of snow-white to grayish chalk or chalky limestone. These sediments are moderately to thickly bedded and include macrofossils such as echinoderms, mollusks, large benthic foraminifera, and calcareous algae. The fossil assemblage confirms a shallow marine, low-energy environment, possibly lagoonal or shelfal in nature [22].

### 2.2. The Madmoud Formation (Pliocene).

According to [23], this unit is divided into two parts: The upper section includes brown to yellow siltstones, sandstones, and claystones deposited under fluvial conditions. The lower section consists of interbedded clay, silt, and fine sandstone, representing floodplain and deltaic settings. These sediments reflect significant fluvial aggradation during Pliocene River reactivation, likely driven by tectonic uplift or base-level changes in the Nile system.

### 2.3. The Issawia Formation (Upper Pliocene to Pleistocene).

This formation comprises clastic facies of gravels, cobbles, and pebbles, often embedded in limestone-rich marls and tufa deposits. The clasts are largely carbonate in origin, including travertine and limestone, suggesting alluvial fan or wadi deposition. Interbedded tufa and carbonates indicate local spring activity or shallow lacustrine deposition [24].

### 2.4. The Armant Formation (Pleistocene).

This formation is composed of alternating beds of fine clastics and carbonate-rich travertine. These indicate periods of clastic fluvial input interrupted by spring carbonate precipitation. The formation reflects episodic sedimentation in a tectonically influenced valley with localized spring discharge [23].

### 2.5. The Qena Formation (Pleistocene).

A prominent unit of cross-bedded gravels and sands, reflecting a high-energy braided river system. The fluviatile nature and semi-consolidated state of the sediments are consistent with a dynamic fluvial regime during pluvial periods of the Pleistocene, when the Nile and its tributaries carried a high sediment load [25].

### 2.6. The Abbassia Formation (Pleistocene).

This formation consists of conglomerates formed of quartzite, granitic, and siliceous limestone fragments in a red sandy matrix. It represents high-energy fluvial processes capable of transporting large clasts over short distances, possibly linked to flash floods or tectonically driven erosion phases [23].

### 2.7. Dandara Formation (Pleistocene).

It is composed of massive siltstones and fine sandstones with transitions to gypsiferous claystone. The presence of gypsum and laminated sandstone indicates an arid to semi-arid environment with intermittent evaporitic conditions—likely representing a sabkha or fluvio-lacustrine environment [26]

### 2.8. The Alluvial Deposits (Nile Floodplain) (Holocene).

These deposits consist of fine-grained clay and silt with minor interbeds of sandstone, representing seasonal floodplain deposition by the modern Nile. They are generally dark in color and may contain organic matter, root traces, and signs of human modification in cultivated areas [27].

### 2.9. The Recent Wadi Deposits (Holocene).

The youngest deposits in the study area include brown carbonate-rich wadi sediments, reworked from Eocene formations and redistributed by seasonal flash floods. These poorly sorted gravels and sands reflect high-energy deposition in ephemeral wadi systems active under arid to semi-arid conditions [28].

Floodplain clays of Holocene age likely contributed to the preservation of mudbrick archaeological structures due to their low permeability and stable depositional environment. In contrast, Holocene wadi gravels may have caused post-depositional disturbances through erosional processes or sediment reworking, potentially displacing or damaging archaeological materials.

From strutctural view, The Sohag Basin lies within a structurally active segment of the Nile Valley, shaped by multiple tectonic regimes from the Cretaceous through the Quaternary. According to Sakran et al. [29], the nearby West Beni Suef Basin is characterized by NW–SE oriented normal faults, ENE strike-slip faults, and NE-plunging folds, forming flower structures and horst–graben systems indicative of transtensional deformation. Bosworth et al. [30] further highlight the role of the Red Sea rifting and the 23 Ma Cairo "mini-plume" event in reactivating basement structures across the Western Desert, including zones west of Sohag. More locally, Tawfik and Hassan [31] document a transition from full to half-graben geometries within the Sohag Basin itself, reflecting syn-depositional extensional tectonics during the Late Miocene to Early Quaternary. Mahran [32] supports this interpretation, noting differential subsidence and accommodation space generation linked to basin-margin fault reactivation. Collectively, these structural influences governed sediment distribution, preserved paleosol horizons, and shaped the Plio–Pleistocene stratigraphy of the region.

## 3. Archaeological and historical background

Akhmim, historically known as Ipu or Khent-Min, is one of the oldest cities in Upper Egypt, with a rich archaeological heritage that dates back to the Pharaonic era, approximately six thousand years ago [1]. The city served as a significant religious and administrative center, dedicated to the fertility god Min, who formed a triad with Isis and Horus [3] It was also the capital of the Ninth Nome of Upper Egypt [2]. Numerous artifacts, such as statues, steles, and temple ruins, have been unearthed during excavations, underscoring the city's importance during the Old Kingdom and later periods. However, the ancient monuments of Akhmim are limited, as the modern city has been built over the original settlement. Notable discoveries include a colossal statue of Queen Meritamun, daughter of Ramses II, highlighting Akhmim's significance during the New Kingdom [3]. The archaeological findings from Akhmim offer important insights into ancient Egyptian religious practices, art, and governance.

During the Greco-Roman period, Akhmim, was known as Panopolis, flourished as a center of religion and the arts. The city gained fame for its textile production, particularly for high-quality linen that was exported throughout the Roman Empire. Archaeological evidence from this period includes finely woven textiles and Coptic manuscripts, reflecting Akhmim's cultural and economic vitality [33]. In addition to textile manufacturing, the city was also known for metalworking and shipbuilding [2]. In the Coptic era, Akhmim emerged as an important Christian center, with many churches and monasteries established in the

area. The remains of these structures, along with Coptic art and carvings, attest to the city's key role in the spread of Christianity in Egypt.

Akhmim's necropolis, situated on the eastern bank of the Nile, includes the tombs of high-ranking officials, underscoring the city's spiritual and political importance. One of the most prominent burial sites is the Hawawish Tombs, located near Akhmim. These tombs primarily date to the Old Kingdom (2686–2181 BCE) and the First Intermediate Period (2181–2055 BCE), making them some of the earliest known burial grounds in the region [34]. Carved into limestone cliffs, the tombs served as final resting places for elite members of Akhmim society, including priests and administrators. The artistic style found in the Hawawish Tombs reflects a blend of traditional Egyptian themes and local influences [35].

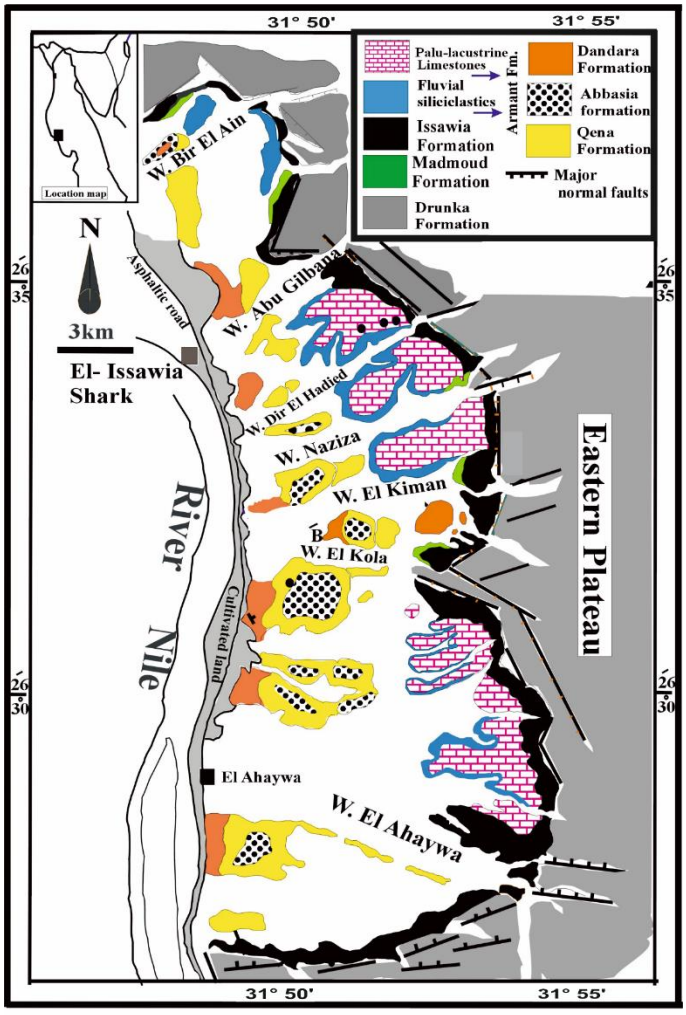


**Figure 3:** Geological map of the study area, modified after [28].

In February 2018, the Egyptian Ministry of Antiquities announced the discovery of the tomb of the priest Tutu at the Al Dayabat archaeological site near Akhmim in Sohag Governorate. The tomb was uncovered by chance when a group of looters was apprehended while digging illegally in the area. Considered one of the most significant archaeological discoveries in recent years, the tomb dates to the Ptolemaic period (305–30 BCE) and offers critical insights into the religious and cultural practices of that era (Fig. 4). The structure includes a central hall with a burial shaft leading to two chambers. Its walls are adorned with vivid and remarkably well-preserved reliefs and inscriptions that shed light on the art and iconography of the Ptolemaic period [21].

This discovery holds several important implications. Historically, it illustrates the cultural fusion between Egyptian and Hellenistic traditions during the Ptolemaic rule. Religiously, it emphasizes the ongoing role of priests in upholding rituals and practices, as seen in the depictions of deities like Isis, Osiris, and Horus, which reflect the enduring nature of ancient Egyptian religious beliefs.

## 4. Methodology

Magnetic surveying has become an essential tool in the scientific investigation of archaeological sites. First introduced in the 1950s [36], it has since evolved into one of the primary methods used in archaeological prospection [11]. Magnetic surveys are commonly used to detect spatial variations in the Earth's magnetic field caused by local differences in total magnetization [37]. By interpreting these magnetic anomalies, it is possible to identify the presence of buried archaeological features [38]. This process relies on a distinct magnetic contrast between the archaeological structures and the surrounding soil or bedrock [39]. Such contrast may arise either naturally or as a result of human activity. Typical anthropogenic sources include soil-filled trenches, intrusive features like walls and foundations, as well as fireplaces, pottery, and bricks [13, 40] This technique offers a fast and effective means of mapping the distribution of archaeological remains in the shallow subsurface [41 – 43].

**Figure 4:** Photographs from media of the excavated tombs of Priest Tutu in 2018 and its wonderful painting in walls beside the stone coffins and some of its antiques.

### 4.1. Data Acquisition

In this study, the selected site was surveyed using a GEM GSM-19 Overhauser magnetometer with a dual-sensor configuration. The lower sensor was positioned at a height of

1.5 meters above ground level, while the upper sensor was mounted 0.6 meters above the lower one (Fig. 5). The choice of the 1.5 m sensor height represents a balance between reducing surface noise and ensuring sufficient sensitivity to shallow subsurface archaeological features. The instrument, owned by the Geology Department at Sohag University, has a high sensitivity of 0.022 nT and a resolution of 0.01 nT, making it well-suited for archaeological prospection. To guarantee high-quality data, the operator maintained a noise-free condition by avoiding any ferromagnetic objects, and the selected site was carefully inspected to ensure the absence of metallic debris that might affect the measurements.

The survey was conducted over a 50 × 50 meters grid, covering a total area of 2,500 square meters. Data acquisition was carried out along survey lines oriented in the NW–SE direction, using a zigzag pattern to optimize field efficiency and minimize survey time (Fig. 6). The inline spacing between traverses was 1 meter, and the device was operated in continuous mode, recording data at 2-second intervals, resulting in a total of 1,250 readings. The outputs of the survey included: Total Magnetic Intensity (TMI) recorded by the lower sensorand Vertical Magnetic Gradient (VMG) calculated as the difference between the upper and lower sensor readings, divided by their vertical separation [44].

**Figure 5:** Photographs of field work of magnetic survey using GEM GSM-19 Overhauser magnetometer with two sensors; the lower sensor hight is 1.5m from the ground. The operator is free from any metallic objects that can affect the magnetic readings.

It is important to note that no base station was used and diurnal correction was not applied. This decision was based on the short duration of the daily field sessions (typically one hour), which were conducted during magnetically quiet periods

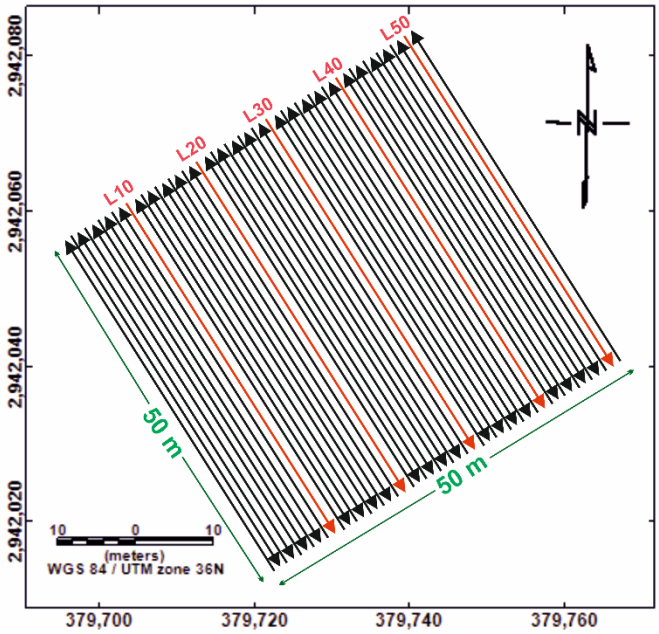


**Figure 6:** Survey layout (50×50 m grid; NW-SE lines; 1 m spacing; line's length is 50m; total number of lines is 51).

based on regional geomagnetic observatory data. Given the small size of the survey area and the objective of detecting local, shallow archaeological anomalies, the lack of diurnal correction is not expected to significantly impact the data quality. Nonetheless, this is acknowledged as a methodological limitation.

### 4.2. Data Processing

All magnetic data were processed using the Geosoft Oasis Montaj software package, version 8.4 [45]. These processing steps were performed to enhance data quality and, as much as possible, to emphasize the archaeological features present within the studied sites.

The processing steps can be summarized as follows:

A high-pass filter was employed on the Total Magnetic Intensity (TMI) data in the frequency domain to enhance the resolution of shallow subsurface features. This type of filter is known for its smooth frequency response and minimal distortion, making it ideal for geophysical applications where data clarity is crucial. The filter was designed with a cutoff wavelength of 10 meters, meaning that magnetic anomalies with wavelengths longer than 10 meters, typically associated with deeper or regional sources, were progressively attenuated [45]. By applying this filter, the TMI data was refined to emphasize localized and subtle magnetic variations, aiding in the detection and interpretation of shallow potentially buried features.

Gradient-based or derivative techniques are widely used in magnetic data processing to enhance the visibility of anomalies, particularly those originating from shallow subsurface sources [46]. These methods work by emphasizing rapid spatial changes in the magnetic field, thereby suppressing broad, regional trends and highlighting more localized variations. Among the different derivative techniques, the vertical derivative is particularly

effective at isolating local anomalies. It is inherently more responsive to near-surface features and less influenced by deeper, large-scale geological structures. This makes it a valuable tool for applications such as archaeological prospection and shallow geological mapping.

The first vertical derivative (FVD) and second vertical derivative (SVD) are commonly applied to magnetic datasets to sharpen anomaly edges and improve spatial resolution. These derivatives enhance the contrast between magnetic sources and the surrounding background, making it easier to delineate small or subtle features. However, it is important to note that while these methods enhance shallow signals, they can also magnify high-frequency noise present in the data [47,48]. Therefore, careful data pre-processing and filtering are essential to balance signal enhancement with noise suppression.

The Analytic Signal (AS), also referred to as the total gradient [45], is a powerful magnetic data transformation technique that combines the horizontal and vertical derivatives of a magnetic anomaly into a single scalar quantity. This composite signal yields a distinct and interpretable shape directly over the source body, providing insights into the location and geometry of subsurface structures. One of the key advantages of the AS is that its amplitude is determined by the spatial coordinates, specifically, the horizontal position and depth of the causative body, while being independent of the direction of magnetization [49]. This insensitivity to magnetization orientation makes the AS especially useful in complex geological or archaeological contexts where the remanent magnetization might vary or be unknown [5].

As a result, the analytic signal serves as a robust tool for locating and characterizing magnetic sources, offering reliable information about their depth, shape, and lateral extent. Its application enhances interpretation accuracy, particularly in areas where directional magnetization effects could otherwise complicate anomaly analysis [50].

The Source Parameter Imaging (SPI) technique is a fast, simple, and highly effective method for estimating the depths of magnetic source bodies. It operates by analyzing the shape and amplitude of magnetic anomalies to compute depth solutions, and has proven to be both efficient and reliable. According to [51], the SPI method achieves an accuracy level of approximately ±20%, as validated through comparisons with drill hole data and other ground-truth sources. This level of precision places SPI on par with more complex techniques such as Euler deconvolution, yet it provides some notable advantages. In particular, SPI tends to generate a denser and more coherent distribution of depth solutions, which contributes to a clearer understanding of subsurface structure [52]. Moreover, the technique is designed with practical usability in mind: its output is typically presented in a format that can be readily interpreted by geoscientists familiar with local geology.

One of the core strengths of SPI lies in its user-friendly implementation, which allows it to be applied efficiently in a variety of geophysical studies. It enables geologists and geophysicists to extract meaningful insights about subsurface features and structural variations without requiring extensive parameter tuning or complex processing steps, making it a valuable tool in both exploration and academic research contexts.

The 3D Euler Deconvolution (ED) method is a derivative-based technique that uses both horizontal and vertical derivatives to achieve two main objectives: identifying the lateral edges of magnetic sources and estimating the depth to the top of sources with significant magnetic contrast [53,54]. Accurate application of this method requires careful selection of several parameters, including grid spacing, data spacing, structural index (SI), and window size [55]. Among these, the structural index and window size are considered the most important. The SI reflects a simplified geological model based on local geological conditions [10]. The window size controls the maximum depth that can be imaged, typically about half the window length [55]. If the window is too small, long-wavelength anomalies may be excluded, making it difficult to estimate their depths [10].

## 5. Results and Discussion:

The total magnetic intensity (TMI) of the study area (Fig. 7a) reveals a relatively low magnetic gradient, with values ranging from 42,417 to 42,440 nT. The highest magnetic readings are concentrated in the southwestern part of the site, gradually decreasing towards the northeast. This initial observation provides a broad overview of the magnetic landscape.

Further interpretation through the vertical magnetic gradient (VMG) map (Fig. 7b) presents an alternating pattern of negative and positive values, ranging from -0.89 to 1.33 nT/m. Significantly, the positive anomalies on this map also exhibit elongated shapes, reinforcing the hypothesis that they correspond to mudbrick walls or their remnants. The VMG technique effectively accentuates the vertical changes in the magnetic field, making these linear features more prominent.

To enhance and isolate more subtle magnetic anomalies, a high-pass filter was applied to the TMI data using a 10-meters cut-off wavelength. The resulting residual magnetic anomaly map (Fig. 7c) clearly delineates distinct oval and semicircular negative anomalies scattered across the study site. These negative anomalies are notably encircled by elongated positive magnetic values, which are interpreted as potential indicators of mudbrick walls. Such formations could represent various tombs, either directly excavated into the ground layers or enclosed by mudbrick structures. The high-pass filtered values range from -0.85 to +0.68 nT, highlighting these specific subsurface features. Elongated positive magnetic anomalies, reaching up to +0.68 nT, exhibit geometric dimensions consistent with Ptolemaic-period mudbrick wall widths, typically ranging between 0.8 and 1.2 meters [5, 6, 18, 19, 56]. In contrast, negative anomalies as low as –0.85 nT are interpreted as tomb voids that have been filled with magnetically low-susceptibility sediments.

To achieve an even more detailed depiction of the subsurface magnetic susceptibility sources, first and second vertical derivatives were applied to the TMI data. The first vertical derivative (FVD) map (Fig. 7d) shows remarkable consistency with the findings from the residual map, with values fluctuating between -1.04 and +0.92 nT/m. This strong correlation validates

the interpretations drawn from the residual data, providing increased confidence in the identified anomalies.

The second vertical derivative (SVD) map (Fig. 7e) is particularly effective at highlighting small, shallow anomalies that might be overlooked by other processing techniques. It also maximizes the boundaries of the distinct negative anomalies, offering a sharper definition of their perimeters. The SVD values range from -1.18 to +0.76 nT/m², further emphasizing the subtle variations in magnetic properties close to the surface. Finally, the analytical signal map (Fig. 7f) showcases distinct, sharp gradient peaks, ranging from 0.178 nT/m to 1.53 nT/m. This method is valuable for precisely locating the edges and centers of magnetic sources, regardless of their magnetization direction. Depth determination was crucial for understanding the three-dimensional extent of the identified features, and two primary methods were employed: source parameter imaging (SPI) and Euler deconvolution.

Inspection of the SPI map (Fig. 8a), derived from the residual data, indicates that the depth to the magnetic sources ranges from 0.5 to 1.5 meter, with an average depth of approximately one meter. This suggests that the anomalies are relatively shallow.

Euler deconvolution was also applied to the residual grid data. The Euler deconvolution map with a structural index (SI) of 0 (Fig. 8b) was used to highlight sharp magnetic contrasts, such as edges of buried walls or foundations, which typically produce contact-like anomalies., revealing depths ranging from less than 0.5 meters to more than 1.5 meters, with a mean depth of one meter. This index is typically used for features like geological contacts or boundaries. For identifying elongated archaeological remains such as walls, roads, foundations, buried trenches or linear ruins, a Euler map with an SI of 1 was generated (Fig. 8c). While showing similar depth limits to the SI=0 map, the mean depth for these linear features was slightly deeper at 1.33 meter. The consistency across these depth estimation methods strengthens the confidence in the derived depths of the subsurface features.

Finally, an interpretive map (Fig. 9) was produced to highlight the most probable locations of archaeological tombs within the study area. This map was constructed using CorelDraw, based on the integration of magnetic maps, including, high-pass filtered and gradient maps. The outlined features, nearly 19 expected tombs, were identified as distinct magnetic anomalies, primarily negative zones enclosed by elongated positive signatures, consistent with buried tombs surrounded by mudbrick structures. While the magnetic interpretation provides strong evidence of subsurface features, confirmation of these findings will require archaeological excavation. This map offers a valuable guide for planning future fieldwork and enhancing the efficiency of archaeological investigations.

## 6. Conclusion

This research successfully demonstrates the value of detailed magnetic prospection in the identification and mapping of shallow-buried archaeological features, particularly in historically rich environments like Akhmim City. The use of a dual-sensor Overhauser magnetometer, coupled with high-density data acquisition and advanced data processing (including high-pass filtering, vertical derivatives, analytic signal, SPI, and Euler Deconvolution), proved highly effective in isolating subtle magnetic anomalies indicative of subsurface structures.

The magnetic anomalies revealed in this study, ranging from circular to elongated forms, are interpreted as possible Ptolemaic tombs and associated mudbrick structures. These features were identified at shallow depths of approximately 0.5 to 1.5 meter. The agreement between SPI and Euler deconvolution results provides robust confirmation of the depth estimates and increases confidence in the reliability of magnetic interpretation in this context. Moreover, the analytic signal enhanced the visibility and geometric interpretation of the sources, regardless of the direction of magnetization, a critical advantage in archaeologically complex settings.

The successful identification of such features in a previously unexcavated area demonstrates the method's ability to direct future archaeological efforts with minimal disruption to the site. This is especially important in areas designated as protected heritage zones, where non-invasive techniques are preferred. The magnetic results not only inform archaeologists about the potential location of tombs of the Ptolemaic period but also assist in reconstructing the site layout.

In summary, this study provides a site-specific methodological and interpretive approach suitable for detecting shallow archaeological features, less than 2 meters, particularly mudbrick walls and voids, under low-magnetic-gradient conditions such as those present in the Al-Diabat area, Sohag. Nineteen expected tombs were correlated based on magnetic results. The method proved to be a cost-effective, non-destructive, and time-efficient tool for identifying subsurface remains in this specific setting. We recommend conducting ground-penetrating radar (GPR) surveys in parallel with magnetic methods for better anomaly characterization and spatial confirmation. Where possible, archaeological excavations are also encouraged to validate geophysical interpretations and ground-truth the results.

## CRediT authorship contribution statement:

Author Contributions: For research articles with several authors, a short paragraph specifying their individual contributions must be provided. The following statements should be used "Conceptualization, Abudeif, A.M. and Mohammed, M.A.; methodology, Gaber, H.A.; software, Gaber, H.A.; validation, Abudeif, A.M., Mohammed, M.A.; and Gaber, H.A.; formal analysis, Gaber, H.A.; investigation, Abudeif, A.M.; resources, Abudeif, A.M.; data curation, Mohammed, M.A.; writing—original draft preparation, Gaber, H.A.; writing—review and editing, Abudeif, A.M.; visualization, Gaber, H.A.; supervision, Abudeif, A.M. and Mohammed, M.A.; project administration, No.; funding acquisition, No. All authors have read and agreed to the published version of the manuscript."

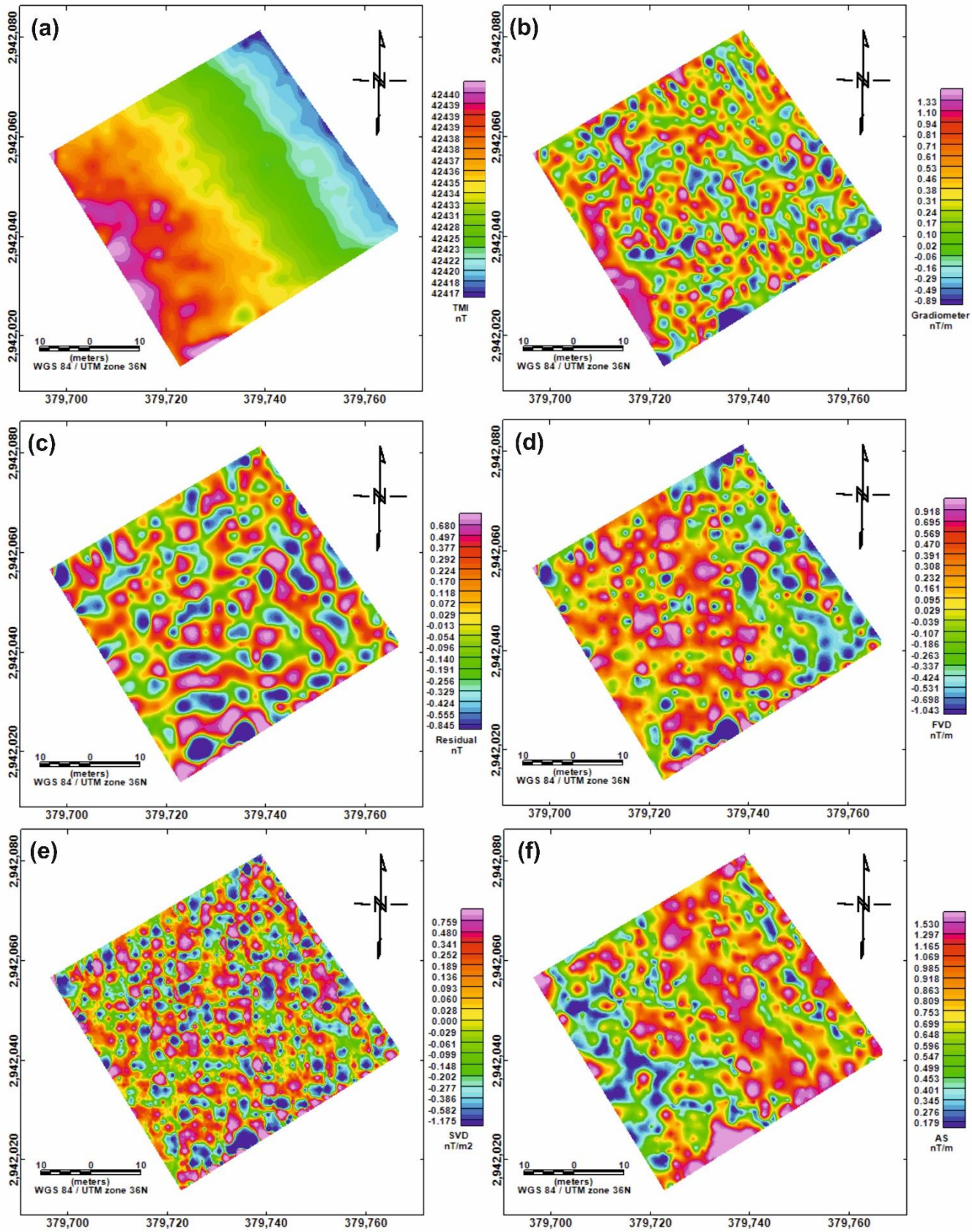


**Figure 7:** Colour maps of magnetic results at the study site; a) Total magnetic intensity (TMI) map of the bottom sensor (42417 nT - 42440 nT), b) Gradiometer magnetic map (-0.89 nT/m – 1.33 nT/m), c) Residual magnetic map (-0.845 nT – 0.680 nT), d) First vertical derivative (FVD) map (-1.043 nT/m – 0.918 nT/m), e) Second vertical derivative (SVD) map (-1.175 nT/m$^2$ – 0.759 nT/m$^2$), and f) Analytical signal (AS) map (0.179 nT/m – 1.530 nT/m).

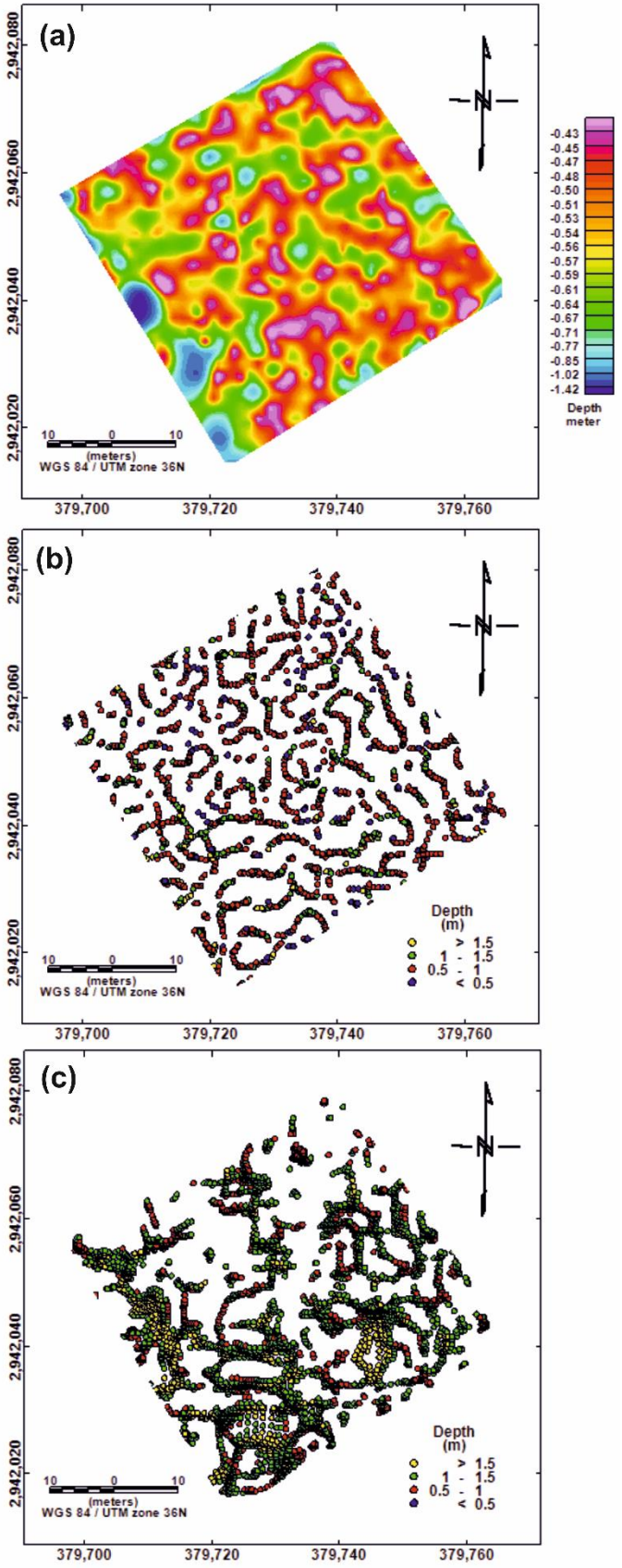


**Figure 8:** Colour maps of depth results of magnetic map (solutions: <0.5–>1.5 m), at the study site; a) Source Parameter Imaging (SPI) map b) Euler Deconvolution map with SI =0, and c) Euler Deconvolution map with SI = 1.

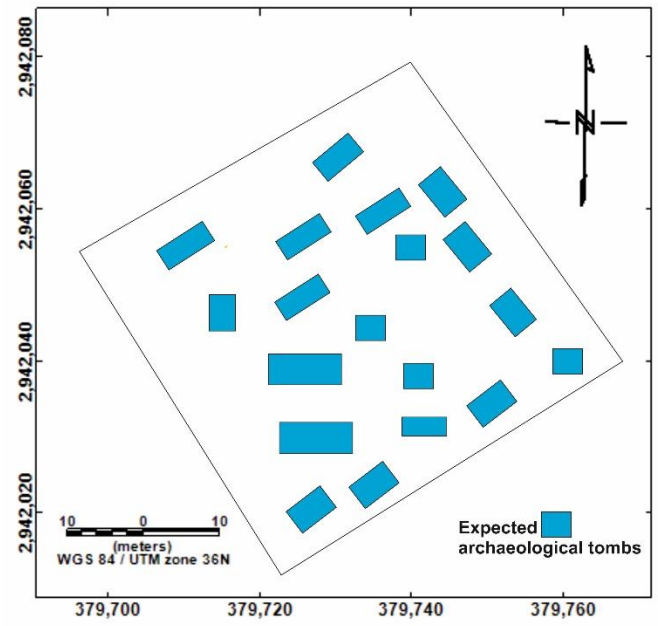


**Figure 9:** A map that outline the possible locations of expected archaeological tombs based on the interpretation of magnetic maps.

## Data availability statement

The data used to support the findings of this study are available from the corresponding author upon request.

## Declaration of competing interest

The authors declare that they have no known competing financial interests or personal relationships that could have appeared to influence the work reported in this paper.

## Acknowledgments

The authors would like to express their special thanks and gratitude to the Egyptian Antiquities Authority for granting us permission to carry out the fieldwork. Also, deep thanks to Geology Department, Faculty of Science, Sohag University for the agreement to use their equipments in data acquisition.

## References

[1] W. Van Rengen, *Panopolis. The Encyclopedia of Ancient History.* Blackwell Publishing Ltd, 2013

[2] M.F. Hafez, *Journal of the Faculty of Tourism and Hotels-University of Sadat City,* 4 (2), (2020) 94-110.

[3] J. Baines, and J. Malek, *Cultural atlas of ancient Egypt.* Checkmark Books, 2000.

[4] A.Y.D.I.N. Büyüksaraç, M.Ö. Arisoy, Ö.Z.C.A.N. Bektaş, Ö. Koçak, and T. Çay, *Archaeological Prospection*, 15(4), (2008) 267-283.

[5] A.M. Abudeif, G.Z. Abdel Aal, J.A. Peláez, R. Sawires, M.M. Masoud, A. Elnassari, K.K. Mansour, H.A. Gaber, and M.A. Mohammed, *Archaeological Prospection*, 32(2), (2024) 459-481.

[6] A.M. Abudeif, G.Z. Abdel Aal, H.S. Ramadan, N. Al-Arifi, S. Bellucci, K.K. Mansour, H.A. Gaber, and M.A. Mohammed, *Sustainability,* 15(14), (2023) p.11119.

[7] A. Khalil, K. Mansour, A. El Kotb, H. Zahra, T.F. Abdallatif, M. Salem, and M. Shaheen, *Geosciences Journal*, 27(5), (2023) 599-611.

[8] A.M. Abudeif, G.Z. Abdel Aal, M.M. Masoud, and M.A. Mohammed, *Applied Sciences*, 12(19), (2022) p.9640.

[9] T. Herbich, *Spuren der altägyptischen Gesellschaft. Festschrift für Stephan J. Seidlmayer. Berlin: de Gruyter*, (2022) 385-407.

[10] A. Ibrahim, M.M. Senosy, A. El-Khadragy, S.A. Saada, K. Abdelrahman, S.S. Alarifi, and K. Mickus, *Journal of Geophysics and Engineering*, *19*(4), (2022) 876-896.

[11] A.E. El Emam, A. Lethy, A.M. Radwan, and A. Awad, *Frontiers in Earth Science*, *9*, (2021) p.674953.

[12] S.B. Ahmed, R.A. El Qassas, and H.F.A. El Salam, *The Egyptian Journal of Remote Sensing and Space Science,* 23(3), (2020) 321-332.

[13] G. El-Qady, M. Metwaly, and M.G. Drahor, *Archaeogeophysics* New York, NY: Springer, 2019.

[14] T. Abdallatif, H.H. Odah, A.E. El Emam, and A. Mohsen,. *Archaeogeophysics: State of the Art and Case Studies,* (2019) 137-168.

[15] B. Gavazzi, R. Alkhatib-Alkontar, M. Munschy, F. Colin, and C. Duvette, *Archaeological prospection*, 24(1), (2017) 59-73.

[16] M. Mekkawi, T. Arafa-Hamed, and T. Abdellatif, *NRIAG Journal of Astronomy and Geophysics,* 2(1), (2013) 175-183.

[17] A.M. Abbas, T.F. Abdallatif, F.A. Shaaban, A. Salem, and M. Suh, *Geoarchaeology: An International Journal*, *20*(5), (2005) 537-554.

[18] T.F. Abdallatif, E.M. Abd-All, M. Suh, R. M. Mostafa and I.A. El-Hemaly, *Geoarchaeology,* 20(5), (2005) 483-503.

[19] T.F. Abdallatif, S.E. Mousa, and A. Elbassiony, *Archaeological Prospection,* 10(1), (2003) 27-42.

[20] H. Ghazala, A.S. El-Mahmoudi, and T.F. Abdallatif,. *Archaeological Prospection,* 10(1), (2003)43-55.

[21] M. H. Marey and A. Abo El-Yamin, *Surface and Interface Analysis*, *53*(1), (2021) pp.31-45.

[22] Z.R. El-Naggar, *The 7th Arab Petroleum Congress, Kuwait,* 64, (1970) 1-50.

[23] R. Said, *The geological evolution of the River Nile.* Springer New York, NY, 1981.

[24] T.M. Mahran, *Qatar University Science Journal* (1995).

[25] B. Issawi, and J. F. Mccauley, *The Followers of Horus, Egypt: Studies Assoc. Public,* (1992) 121-138.

[26] R. Said, *The Geology of Egypt*, 734. Rotterdam, Brookfield, A.A. Balkema, 1990.

[27] A. Omer, *Geological, mineralogical and geochemical studies on the Neogene and Quaternary Nile basin deposits, Qena-Assiut stretch, Egypt.* Ph. D. thesis, Geology Dept. Faculty of Science, Sohag, South Valley University, 1996.

[28] B. EL-Haddad, *Evolution of the geological history of the Egyptian Nile at Sohag area using sedimentological studies and remote sensing techniques.* Geology dept., Faculty of Science, Sohag University, 2014.

[29] Sh. Sakran, A.A. Shehata, O. Osman, M. El Sherbiny, *Journal of African Earth Sciences* 154, (2019) pp. 1–19.

[30] W. Bosworth, D.F. Stockli, D.E. Helgeson, *Journal of African Earth Sciences* 109, (2015) pp. 107–119.

[31] T. Mahran, and A.M. Hassan, *Journal of African Earth Sciences*, 199, (2023) p.104829.

[32] T. Mahran, *Arabian Journal of Geosciences,* 17(9), (2024) p.250.

[33] C. Riggs, *The beautiful burial in Roman Egypt: art, identity, and funerary religion,* OUP Oxford. 2006.

[34] E. M. Thompson, *A study of the architecture of the cemetery of El-Hawawish at Akhmim in Upper Egypt in the Old Kingdom.* Macquarie University, 2002.

[35] N. Kanawati, *The tomb and beyond: Burial customs of Egyptian officials*, Oxbow Classics in Egyptology 144 p, 2024.

[36] M.J. Aitken, *Contemporary Physics*, 3(5), (1962) 334-352.

[37] A. Schmidt, P. Linford, N. Linford, A. David, C. Gaffney, A. Sarris, and J. Fassbinder, EAC guidelines for the use of geophysics in archaeology: questions to ask and points to consider. EAC Guidelines 2, Europae Archaeologia Consilium (EAC), Association Internationale sans But Lucratif (AISBL), Namur, Belgium, 137 p, 2015.

[38] I.M. Ibraheem, R. Bergers and B. Tezkan, *Near Surface Geophysics,* 19(5), (2021) 603-623.

[39] R. Di Maio, M. La Manna, and E. Piegari, *Archaeological Prospection,* 23(1), (2016) 3-13.

[40] S. Piro, Introduction to geophysics for archaeology. In Seeing the unseen. Geophysics and landscape archaeology (pp. 53-92). CRC Press, 2008.

[41] A.J. Clark, *Geophysics*, 51(7), (1986) 1404-1413.

[42] I. Scollar, A. Tabbagh, A. Hesse and I. Herzog, *Archaeological prospecting and remote sensing* (p. 674). Cambridge University Press. 1990.

[43] J.M. Reynolds, *An introduction to applied and environmental geophysics.* John Wiley & Sons, 2011.

[44] J.D. Phillips, *SEG Technical Program Expanded Abstracts* (2000) 402-405.

[45] Geosoft oasis montaj, V.8.4. Geosoft Software for the Earth Science, Geosoft Inc., Toronto, Canada, 2015.

[46] I. Marson, and E.E. Klingele, *Geophysics*, 58(11), (1993) 1588-1595.

[47] M.N. Nabighian, *Geophysics*, 49(6), (1984) 780-786.

[48] J.D., Fairhead, *Advances in gravity and magnetic processing and interpretation*. Earthdoc. 2015.

[49] S. Qin, *Geophysical Prospecting,* 42(6), (1994) 665-675.

[50] A. Salem, D. Ravat, T.J. Gamey, and K. Ushijima, *Journal of Applied Geophysics,* 49(4), (2002) 231-244.

[51] J.B. Thurston and R.S. Smith, *Geophysics*, 62(3), (1997) 807-813.

[52] R.S. Smith, J.B. Thurston, T.F. Dai and I.N. MacLeod, *Geophysical prospecting*, 46(2), (1998) 141-151.

[53] A.B. Reid, J.M. Allsop, H. Granser, A.T. Millett, and I.W. Somerton, *Geophysics*, 55(1), (1990) 80-91.

[54] P.Y. Stavrev, *Geophysical Prospecting*, 45(2), (1997) 207-246.

[55] A.B. Reid, J. Ebbing, and S.J. Webb, *Geophysical Prospecting*, 62(5), (2014) 1162-1168.

[56] G.Z. Abdelaal, S.K. Abbas, A. M. Abudeif, and M. A. Mohammed, *Assiut University Journal of Multidisciplinary Scientific Research*, *51*(3), (2022) pp.279-308.